GEOLOGY | THE GEOLOGICAL SOCIETY OF AMERICA®

https://doi.org/10.1130/G49061.1

Manuscript received 30 January 2021
Revised manuscript received 17 March 2021
Manuscript accepted 21 June 2021

Published online 12 August 2021

Clear as mud: Clinoform progradation and expanded records of the Paleocene-Eocene Thermal Maximum

Luca G. Podrecca[1,2], Maria Makarova[1], Kenneth G. Miller[1], James V. Browning[1] and James D. Wright[1]

[1]Department of Earth and Planetary Sciences and Institute of Earth, Oceans, and Atmospheric Sciences, Rutgers University, Piscataway, New Jersey 08854, USA

[2]Department of Earth and Planetary Sciences, Northwestern University, Evanston, Illinois 60208, USA

ABSTRACT

The mid-Atlantic coastal plain (eastern United States) preserves high-resolution records of the Paleocene-Eocene Thermal Maximum (PETM) and attendant carbon isotope excursion (CIE), though preservation is highly variable from site to site. Here, we use a dip transect of expanded (as much as 15 m thick) PETM sections from the New Jersey coastal plain to build a cross-shelf PETM depositional model that explains the variability of these records. We invoke enhanced delivery of fine-grained sediments, due to the rapid environmental changes associated with this hyperthermal event, to explain relatively thick PETM deposits. We utilize $\delta^{13}C_{bulk}$, percent $CaCO_3$, and percent coarse fraction (>63 µm) data, supported by biostratigraphic records, to correlate sites along a paleoslope dip transect. Updip cores from Medford, New Jersey, preserve expanded sections of the initiation of the PETM and the earliest portion of the CIE. Medial sites (Wilson Lake, Millville) preserve an expanded CIE body, and downdip Bass River records the CIE recovery. We interpret this pattern to reflect the progradation of clinoform foresets across the paleoshelf via fluid mud, similar to modern high-sediment-supply rivers and adjacent muddy shelves (e.g., the Amazon, Mahakam [Indonesia], and Ayeyarwady [Myanmar] Rivers). Our subaqueous-clinoform delta model explains the pattern of the CIE records and provides a framework for future PETM studies in the region.

INTRODUCTION

The Paleocene-Eocene Thermal Maximum (PETM; 56 Ma) and attendant carbon isotope excursion (CIE) represent the largest warming event and carbon cycle perturbation of the Cenozoic. Global temperatures rose by 4–8 °C (e.g., Kennett and Stott, 1991; Zachos et al., 2003) while $\delta^{13}C$ values decreased by 2‰–4‰ in marine sections (foraminiferal and organic records) and by as much as 7.6‰ in the terrestrial realm (plant lipids) (see McInerney and Wing [2011] for a full review of CIE proxies). Understanding the trigger, rate, and timing of this light-carbon injection is hindered, in part, because most marine CIE-PETM sections are thin (<1 m in 200 k.y.) and thus cannot resolve geologically rapid events (<10 k.y.).

The general structure of the CIE is similar globally, beginning with a sharp drop in $\delta^{13}C$ values that is used to correlate the base of the Eocene (Paleocene-Eocene boundary) from its stratotype in Dababiya, Egypt (Aubry et al., 2007). In deep-sea sections, the $\delta^{13}C$ decrease is sharp (<10 cm), while on continental margin sections, it can be >2 m thick (Figs. 1–3). A sustained interval of low $\delta^{13}C$ values (the body of the CIE) followed the $\delta^{13}C$ decrease and was succeeded by a logarithmic return to near pre-CIE $\delta^{13}C$ values (the recovery; e.g., Dickens et al., 1997; Röhl et al., 2007). The PETM-CIE lasted ~200 k.y. from onset to recovery (Dickens et al., 1997; 170 ± 30 k.y. astronomical estimate of Zeebe and Lourens [2019]).

The warming associated with the PETM coincided with rapid input of fine-grained sediments to the continental shelf along the mid-Atlantic U.S. continental margin. Thick PETM deposits have been reported on the Maryland (e.g., Self-Trail et al., 2017) and New Jersey coastal plains (NJCP) (e.g., Cramer et al., 1999), which provide greater temporal resolution of the onset and body of the CIE compared to deep-marine settings. Rapid mud deposition on the mid-Atlantic paleoshelf during the PETM has been dubbed the "Appalachian Amazon" (Kopp et al., 2009), characterized by energetic, mud-laden riverine transport and subaqueous dysoxic deposition (Stassen et al., 2012). In the NJCP, uppermost Paleocene Vincentown Formation sands and silts are conformably overlain by the kaolinite-rich clays of the lowermost Eocene Marlboro Formation (Gibson et al., 2000; Cramer et al., 1999) that preserve the CIE.

We cored these sediments adjacent to NJCP–PETM outcrops (Medford Auger Project [MAP]; 39.86°N, 74.82°W; Fig. 1; described in the Supplemental Material[1]) and correlate with PETM sections across a transect recovered in International Ocean Discovery Program (IODP) Leg 174AX sites at Wilson Lake (WL hole B; WL hole A was drilled by the U.S. Geological Survey [USGS]), Millville (MV), and Bass River (BR) (Figs. 2 and 3).

These sites each record different parts of the CIE (onset, decrease, body, and recovery) identified by extensive bio- and chemostratigraphic studies (Cramer et al., 1999; Gibbs et al., 2006; Harris et al., 2010; Stassen et al., 2012, 2015; Wright and Schaller, 2013; Makarova et al., 2017). Proximal sites on our transect preserve a notable "transitional unit" that is completely absent in deep-sea sections. This transitional package of sediments preserves the marked shift in grain size, carbonate content, and carbon-isotope geochemistry that signals the rapid change in facies associated with this hyperthermal.

[1]Supplemental Material. Detailed methods including description of the Medford Auger Project, lithostratigraphy and depositional environments, the low-carbonate zone on NJCP, grain size analyses, comparing bulk $\delta^{13}C$ records at MAP and WL, clinoforms, fluid muds, and modern analogs; and Figures S1–S3 (correlation of bulk $\delta^{13}C$ records at MAP and WL and grain size analyses comparisons from the Malvern Mastersizer and from pipette analysis). Please visit https://doi.org/10.1130/GEOL.S.15062313 to access the supplemental material, and contact editing@geosociety.org with any questions.

CITATION: Podrecca, L.G., et al., 2021, Clear as mud: Clinoform progradation and expanded records of the Paleocene-Eocene Thermal Maximum: Geology, v. 49, p. 1441–1445, https://doi.org/10.1130/G49061.1

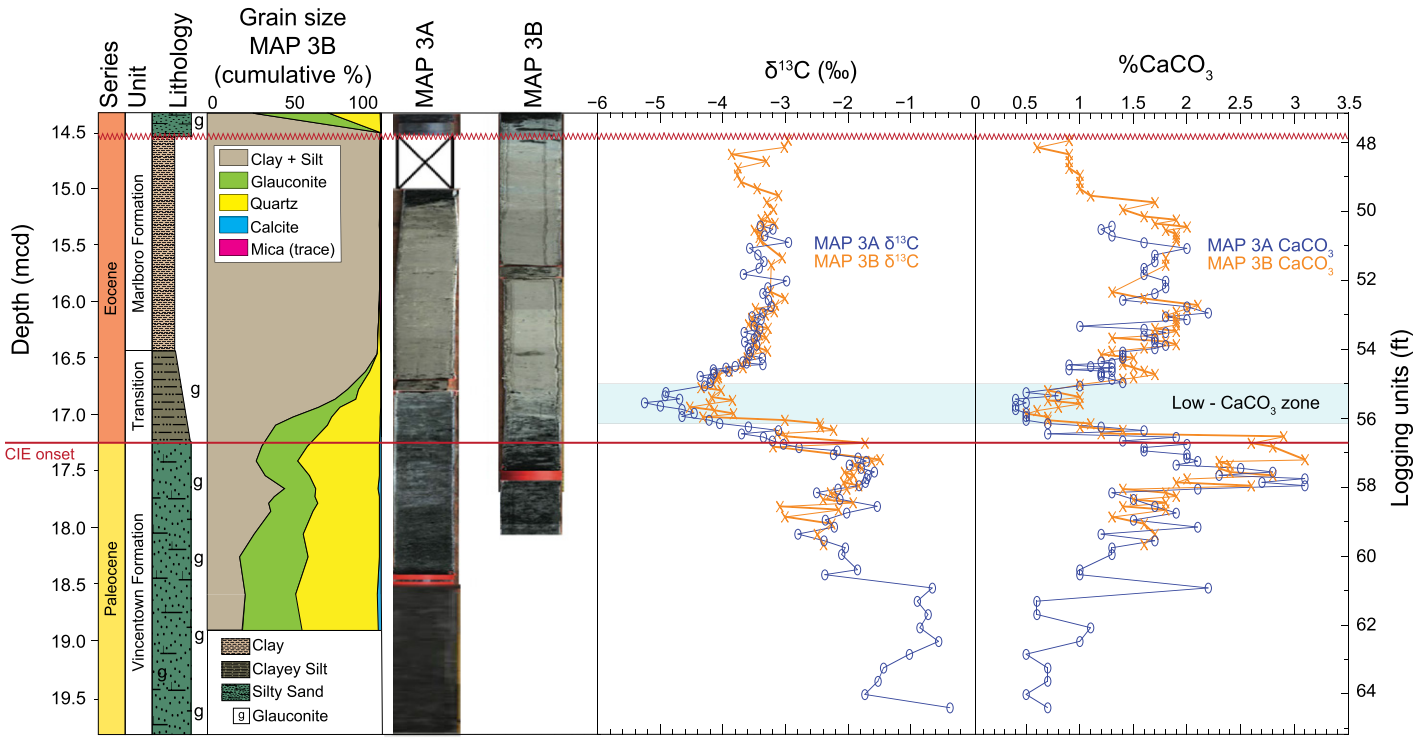

Figure 1. Compilation data for Medford Auger Project (MAP) cores MAP 3A and 3B (New Jersey coastal plain, eastern USA). Lithology, cumulative grain size (displaying relative percent of fines and sand components and authigenic minerals), percent $CaCO_3$, and $\delta^{13}C$ of bulk carbonates (blue for MAP 3A and orange for MAP 3B). Toothed red line represents regional unconformity. The X in the photograph represents sediment missing due to core. Depths are adjusted for core expansion. CIE—carbon isotope excursion; mcd—meters composite depth.

These PETM records are greatly expanded (e.g., the CIE body is >10 m thick at WL and MV; Fig. 3), requiring average sedimentation rates exceeding 12.5 cm/k.y. (with estimates as high as 2 cm/yr; Wright and Schaller, 2013), versus ~4 cm/k.y. background sedimentation rates during Vincentown Formation deposition (Miller et al., 1997).

We evaluate CIE heterogeneity on the mid-Atlantic paleoshelf transect and correlate using $\delta^{13}C_{bulk}$, percent $CaCO_3$, percent coarse fraction (%CF; >63 μm), and nannofossil and benthic foraminiferal biostratigraphy across a paleoslope dip profile spanning 45 km (30–50 m of deepening; Makarova et al., 2017). We do not address the trigger of the PETM, focusing instead on the relationship between rapid warming and sediment input. The differential expression of the CIE across the shelf (shape, thickness, and preserved section at each location) provides a framework of relative time that can later be used to assess proposed mechanisms.

MATERIALS AND METHODS

In 2016, the MAP continuously cored 10 holes at six closely spaced (<1 km) sites in Medford, New Jersey, targeting updip PETM sections (Fig. 2). This study focuses on two adjacent holes, MAP 3A and MAP 3B (<5 m apart), drilled ~700 m downdip of the Marlboro Formation outcrop and the IODP Leg 174AX site at Medford (Sugarman et al., 2010), to construct a complete record for site MAP 3 (Fig. 1). A modified depth scale (i.e. meters composite depth; mcd) is applied to adjust for core expansion and is used for correlation between sites MAP 3A and MAP 3B.

We measured $\delta^{13}C_{bulk}$ and percent $CaCO_3$ on a Fisons Optima mass spectrometer with an attached Multiprep device in the Rutgers University (New Jersey, USA) stable isotope lab. Sediments taken from MAP cores were washed through a 63 μm sieve to determine %CF. Grain-size analysis was initially conducted via laser diffraction on a Malvern Mastersizer 3000, and later via traditional pipette methods (see the Supplemental Material).

RESULTS

Site MAP 3 Facies

The cores from site MAP 3 recovered uppermost Paleocene to lowermost Eocene sands and muds from 14.5 to 19.8 m mcd (Fig. 1). The Vincentown Formation (17.4–19.8 m mcd) is a silty sand interpreted to reflect a lower shoreface facies deposited below fair-weather wave base (see the Supplemental Material). The Marlboro Formation (14.5–16.5 m mcd) is a kaolinitic silty clay (mean grain size <2 μm; Fig. 1; Fig. S2 in the Supplemental Material) deposited in a prodelta setting in middle neritic paleodepths (~30–50 m; see the Supplemental Material). The transitional unit (16.5–17.4 m mcd) between these two formations is defined by rapidly fining-upward sediments (%CF decreases 72% to 2%). This transitional unit also preserves the rapid change in percent $CaCO_3$ (Fig. 1). At site MAP 3, the transitional unit captures the CIE onset and part of the subsequent CIE decrease. This CIE decrease is extremely sharp in open ocean sites, which, in conjunction with the biostratigraphic correlations, suggests far higher rates of sedimentation on the NJCP: 2.7 m of sediment preserves the CIE onset and initial CIE decrease at hole MAP 3B, versus <10 cm in open-ocean sites.

New Jersey Coastal Plain Sites Correlation

We hang our cross-shelf correlation on the CIE onset, which is coincident with the initial decrease in percent $CaCO_3$ (Fig. 2). Our transect shows clear cross-shelf patterns (Fig. 2). The updip MAP and WL sites preserve distinct transitional units and an expanded view of the onset and start of the CIE decrease (Fig. 3). We cannot make quantitative inferences on sedimentation rates, though $\delta^{13}C$ correlations suggest that the onset and decrease sediments recovered at MAP 3 are expanded compared to those at WL (Fig. S1). However, the data sets we have available—comparison of $\delta^{13}C_{bulk}$ records, lithology (uniform silty clay), and benthic assemblages (see below)—argue that site MAP 3 preserves the early part of the CIE decrease and body while the second, more gradual step of the $\delta^{13}C$ decrease (seen elsewhere on the NJCP; Fig. 3; Fig. S1) is absent.

The transitional unit thins downdip at site MV (Wright and Schaller, 2013; Makarova

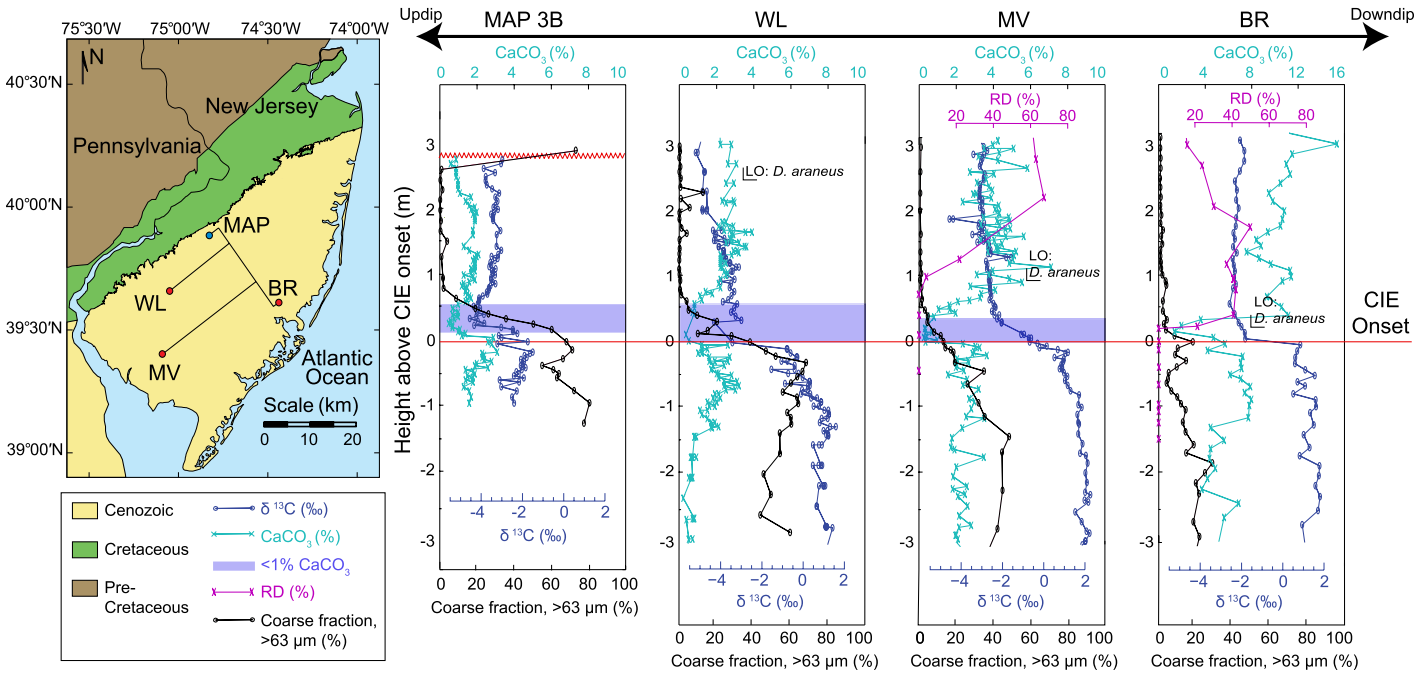

Figure 2. (Left) Site map of New Jersey coastal plain. MAP—Medford Auger Project site; WL—Wilson Lake site; MV—Millville site; BR—Bass River site. (Right) $\delta^{13}C$ (dark blue) and percent $CaCO_3$ (cyan) on downdip transect (Wright and Schaller, 2013; Makarova et al., 2017; Kent et al., 2003; John et al., 2008), and percent coarse fraction (>63 µm; John et al., 2008; Stassen et al., 2015; Makarova et al., 2017) and percent *Rhomboaster-Discoaster* (RD) assemblage (Harris et al., 2010). CIE—carbon isotope excursion; LO—lowest occurrence; *D. araneus*—*Discoaster araneus*.

et al., 2017) and appears to be absent at site BR (Cramer et al., 1999; Fig. 2), where the CIE onset may be diastemic (Stassen et al., 2012). The recovery is apparently completely preserved downdip at site BR, truncated at site MV (Makarova et al., 2017), thin and also incomplete at site WL, and absent updip at site MAP 3 (Fig. 3).

Our correlations are reinforced by biostratigraphy. The CIE body is associated with the *Rhomboaster-Discoaster* (RD) assemblage in the open ocean (Kahn and Aubry, 2004) and in New Jersey (Harris et al., 2010). At downdip sites (MV, BR), the RD assemblage appears at the base of the CIE body, increases sharply to an acme, and decreases in abundance before disappearing in the recovery (Fig. 3; Harris et al., 2010). We do not have access to quantitative data for site WL, however nannofossil biostratigraphy (compiled for hole A in Stassen et al. [2012, 2015] and hole B by Miller et al. [2017]) places the lowest occurrence of *Discoaster araneus* (a marker of the RD assemblage) at the base of the CIE body (Fig. 3). Benthic foraminiferal assemblages at site MAP 3 are characterized by small individual specimens (<212 µm) and dominated by *Anomalinoides acuta* and *Ammobaculites midwayensis* (Makarova, 2018), indicating equivalence to the CIE decrease or body at site WL (Stassen et al., 2015).

DISCUSSION

Subaqueous Clinoform Delta Model

We explain variability of the sediments of the transitional unit and associated CIE onset and decrease across the shelf as the result of a progradational clinoform delta, with thin sigmoidal topsets, thick foresets, and thin bottomsets (Fig. 3). Though the chronology is known only within a relative time scale of several thousand years, the shift in deposition from site MAP to site WL during the CIE onset and decrease resulted in a 9 km seaward progradation (Fig. 3) in $\leq$ 4 k.y. (using the chronology of Zeebe and Lourens [2019]) and perhaps much faster (using the chronology of Wright and Schaller [2013]).

Evidence for rapid, mud-laden riverine transport and high sedimentation rates includes the lack of bioturbation, physical remnants (vertical sticks and leaves; e.g., Wright and Schaller, 2013), biofacies assemblages (Stassen et al., 2012, 2015), and magnetofossils at least partly indicative of dysoxic environments (Kopp et al., 2009; Wang et al., 2015).

In our model, muds originating from the Appalachians, Piedmont, and coastal plain built individual chronostratigraphic units, each preserving a different "snapshot" of the CIE. The earliest packages of fining-upward sand to mud (transitional unit) and overlying clay (Marlboro Formation) captured the CIE onset and initial part of the $\delta^{13}C$ decrease (Fig. 3). As accommodation space filled, fluid mud transport drove delta progradation seaward, allowing subsequent clinoform deposition to record the CIE body and recovery (Fig. 3). Meanwhile, updip sections were bypassed and truncated as the seafloor intersected wave base. This produced a regional unconformity capping the Marlboro Formation (Fig. 3; e.g., Gibson et al., 2000). Volume scaling suggests that Amazon shelf–like conditions on the mid-Atlantic coastal plain would have required ~25% of the modern Amazon sediment flux during the PETM (Kopp et al., 2009).

Inferring paleoenvironmental conditions via stratigraphic correlation is subject to some uncertainty due to spatiotemporal variability in sedimentation rates and autocyclical shifts in depocenters (e.g., Trampush and Hajek, 2017; Foreman and Straub, 2017). However, the biostratigraphic, chemostratigraphic, and lithologic trends demonstrated in this study (Fig. 2) are consistent with our progradational depositional model, whether that trend is predicted to disappear proximally and expand in a downdip direction (CIE body and recovery, percent RD influx [the sediments preserving the appearance of RD]) or, in contrast, disappear distally with expanded sections updip (CIE decrease, low-carbonate zone). We acknowledge that our sedimentary records may not be complete, which could have resulted in an incomplete depiction of a three-dimensional, lobe-shaped geometry on our two-dimensional cross section. However, the consistent patterns observed across the transect (Figs. 2 and 3) support this general pattern of sedimentation.

This rapid progradational mud system explains the relative distribution of biofacies, the variable expression of the CIE, and the lithology on the NJCP. The high sedimentation rates on the mid-Atlantic paleoshelf have been attributed to the warm subtropical PETM climate, analogous to that of the modern Amazon (e.g., Nittrouer

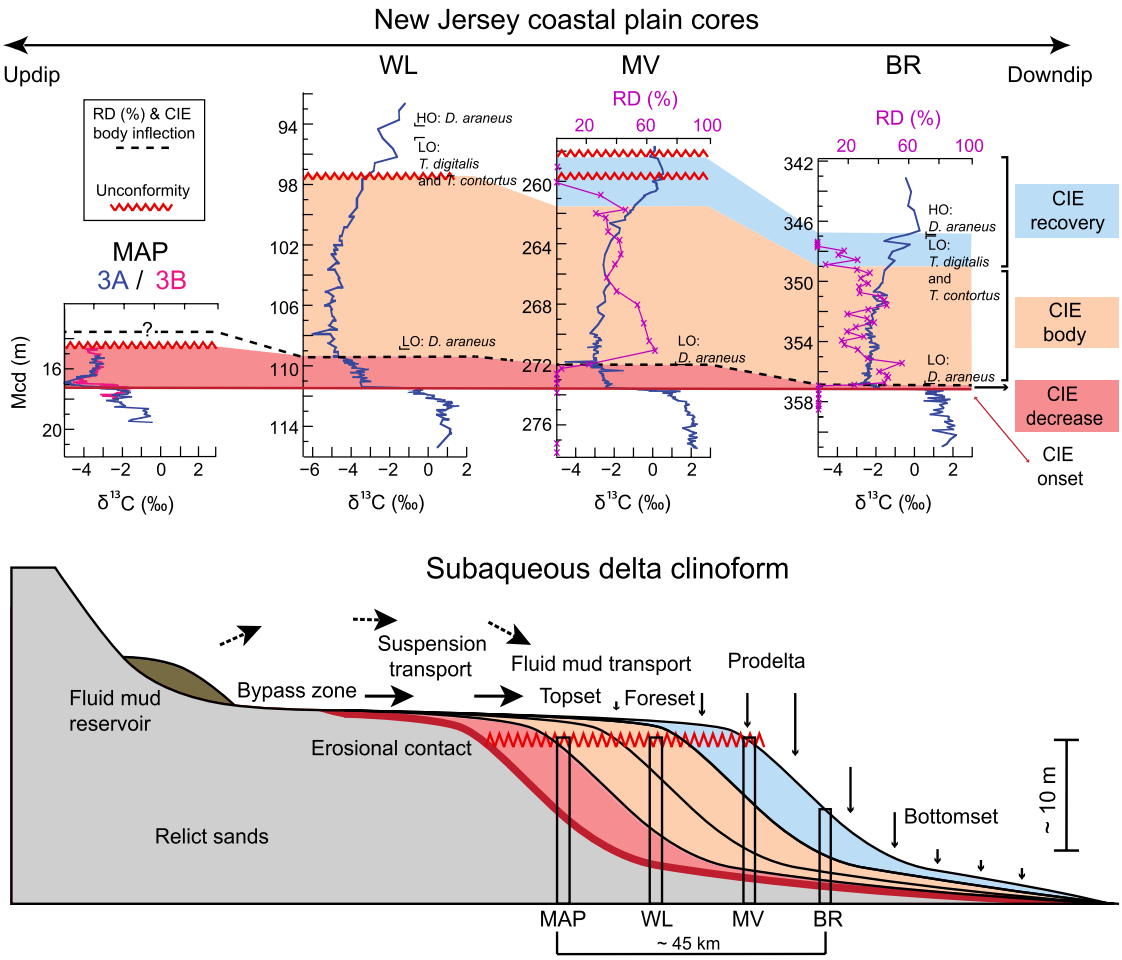

Figure 3. (Top) Bulk $\delta^{13}C$ records across four New Jersey coastal plain sites: Medford Auger Project (MAP) site, holes 3A (blue) and 3B (pink); Wilson Lake (WL) site, hole B (Wright and Schaller, 2013); Millville (MV) site (Makarova et al., 2017); and Bass River (BR) site (Cramer et al., 1999; John et al., 2008). Also shown are percent *Rhomboaster-Discoaster* (RD) assemblage (Harris et al., 2010 [MV and BR]; Miller et al., 2017 [WL]) and benthic biostratigraphy (Stassen et al., 2015). mcd—modified composite depth; LO—lowest occurrence; HO—highest occurrence. *Rhomboaster/Discoaster*; *D. araneus*—*Discoaster araneus*; *T. digitalis*—*Tribrachiatus digitalis*; *T. contortus*—*Tribrachiatus contortus*. Records are aligned on carbon isotope excursion (CIE) onset (straight red line), correlated with biostratigraphy, and presented with uniform vertical scale. Note WL $\delta^{13}C$ record is from hole B, while benthic biostratigraphy is from hole A; there is 1.5–1.8 m offset between holes (Miller et al., 2017), accounted for in the graphic. (Bottom) Idealized subaqueous delta clinoform depositional model depicting fluid mud reservoir source bypassing shallow zones and rapidly building foresets in prodelta environment. Red saw-toothed line denotes unconformity capping top of Marlboro Formation.

et al., 1995) and other high-input rivers (e.g., Mahakam [Indonesia], Ayeyarwady [Myanmar]). Modern subaqueous clinoform deltas are associated with large mud-laden riverine systems around the globe, including the Ganges-Brahmaputra (India and Bangladesh; Kuehl et al., 2005), Fly (Papua New Guinea; Walsh et al., 2004), Yangtze (China; Chen et al., 2000), Mahakam (Storms et al., 2005), and Ayeyarwady (Liu et al., 2020) Rivers. These delta systems all share two critical conditions: high input of muddy riverine sediments, and an energetic tide- or storm-dominated environment to facilitate transport.

In particular, we identify the Holocene Amazon, Mahakam, and Ayeyarwady river systems as important case studies for drawing modern analogs for the Marlboro Formation clinoforms. Observations in these systems detail how muds coalesce and accumulate in topset depocenters under tidal and wave forces and are then episodically transported across the shelf by fluid mud processes (e.g., on the Amazon delta; Kineke et al., 1996). Using these analogs, we invoke rapid fluid mud deposition as the transport mechanism for delta mud clinoforms on the NJCP during the PETM.

Cross-shelf movement of fluid mud requires an energetic transport mechanism (i.e., tides or storms). On the Holocene storm-dominated mid-Atlantic continental shelf, clay sediments are trapped in estuaries, while mud that reaches the shelf is swept into the deep sea by energetic storms (Miller et al., 2014). Though the PETM differed climatologically (lower latitudinal gradients), the high supply of mud accumulated in the shallow embayment, where storms and tides facilitated transport to the foresets and bottomsets, as observed in modern mud-rich systems (Nittrouer et al., 1995; Storms et al., 2005; Liu et al., 2020).

Our PETM depositional model suggests progradation rates similar to those observed in Holocene high-sediment-supply river systems. For example, the Holocene Mahakam delta has prograded ~60 km into the Makassar Strait over the past 5000 yr (~12 km/k.y.; Storms et al., 2005), while our model suggests 45 km of progradation during the geologically brief PETM (Fig. 3). Thus, we incorporate modern studies of muddy river systems to evaluate the distribution of these PETM clays. This approach provides a mechanism that explains the variability in the preservation of the CIE in this region and a blueprint for planning future studies.

CONCLUSIONS

Geochemical, sedimentological, and biostratigraphic records demonstrate that deposition on the New Jersey paleoshelf during the PETM consisted of prograding depocenters. A strengthened hydrological cycle bolstered riverine transport of muds to the paleoshelf. We explain the variability of the CIE records observed on our cross-shelf transect using a progradational clinoform depositional model supported by cross-shelf correlations of multiproxy lithologic, biostratigraphic, and $\delta^{13}C_{bulk}$ data. Proximal (updip) sites record high fluxes of sediments during the CIE onset, which rapidly filled available accommodation space, forcing clinoforms to prograde into deeper water. Our PETM progradational model illuminates the influence of transient warming events on continental shelves and presents a qualitative chronostratigraphic tool for correlating PETM sites across the mid-Atlantic paleoshelf and for selecting future drill-site locations based on CIE target intervals.

ACKNOWLEDGMENTS

We thank the late C. Lombardi, who proposed the possibility of fluid mud deposition on the New Jersey coastal plain during the PETM; the U.S. Geological Survey drillers, particularly the late J. Grey, for their efforts; the International Ocean Discovery Program for samples from Leg 174AX sites; as well as the anonymous reviewers who, alongside Elizabeth Hajek, contributed feedback that greatly enhanced the strength of this paper. This work was supported by U.S. National Science Foundation grants OCE16-57013 (Miller) and OCE14-63759 (Miller and Browning).

REFERENCES CITED

Aubry, M.-P., Ouda, K., Dupuis, C., Berggren, W.A., and Van Couvering, J.A., and the Members of the Working Group on the Paleocene/Eocene Boundary, 2007, The Global Standard Stratotype-section and Point (GSSP) for the base of the Eocene Series in the Dababiya section (Egypt): Episodes, v. 30, p. 271–286, https://doi.org/10.18814/epiiugs/2007/v30i4/003.

Chen, Z.Y., Song, B.P., Wang, Z.H., and Cai, Y.L., 2000, Late Quaternary evolution of the subaqueous Yangtze Delta, China: Sedimentation, stratigraphy, palynology, and deformation: Marine Geology, v. 162, p. 423–441, https://doi.org/10.1016/S0025-3227(99)00064-X.

Cramer, B.S., Aubry, M.-P., Miller, K.G., Olsson, R.K., Wright, J.D., and Kent, D.V., 1999, An exceptional chronologic, isotopic, and clay mineralogic record at the latest Paleocene thermal maximum, Bass River, NJ, ODP 174AX: Bulletin de la Société Géologique de France, v. 170, p. 883–897.

Dickens, G.R., Castillo, M.M., and Walker, J.C.G., 1997, Blast of gas in the latest Paleocene: Simulating first-order effects of massive dissociation of oceanic methane hydrate: Geology, v. 25, p. 259–262, https://doi.org/10.1130/0091-7613(1997)025<0259:ABOGIT>2.3.CO;2.

Foreman, B.Z., and Straub, K.M., 2017, Autogenic geomorphic processes determine the resolution and fidelity of terrestrial paleoclimate records: Science Advances, v. 3, e1700683, https://doi.org/10.1126/sciadv.1700683.

Gibbs, S.J., Bralower, T.J., Bown, P.R., Zachos, J.C., and Bybell, L.M., 2006, Shelf and open-ocean calcareous phytoplankton assemblages across the Paleocene-Eocene Thermal Maximum: Implications for global productivity gradients: Geology, v. 34, p. 233–236, https://doi.org/10.1130/G22381.1.

Gibson, T.G., Bybell, L.M., and Mason, D.B., 2000, Stratigraphic and climatic implications of clay mineral changes around the Paleocene/Eocene boundary of the northeastern US margin: Sedimentary Geology, v. 134, p. 65–92, https://doi.org/10.1016/S0037-0738(00)00014-2.

Harris, A.D., Miller, K.G., Browning, J.V., Sugarman, P.J., Olsson, R.K., Cramer, B.S., and Wright, J.D., 2010, Integrated stratigraphic studies of Paleocene–lowermost Eocene sequences, New Jersey Coastal Plain: Evidence for glacioeustatic control: Paleoceanography, v. 25, PA3211, https://doi.org/10.1029/2009PA001800.

John, C.M., Bohaty, S.M., Zachos, J.C., Sluijs, A., Gibbs, S., Brinkhuis, H., and Bralower, T.J., 2008, North American continental margin records of the Paleocene-Eocene thermal maximum: Implications for global carbon and hydrological cycling: Paleoceanography, v. 23, PA2217, https://doi.org/10.1029/2007PA001465.

Kahn, A., and Aubry, M.-P., 2004, Provincialism associated with the Paleocene/Eocene thermal maximum: Temporal constraint: Marine Micropaleontology, v. 52, p. 117–131, https://doi.org/10.1016/j.marmicro.2004.04.003.

Kennett, J.P., and Stott, L.D., 1991, Abrupt deep-sea warming, palaeoceanographic changes and benthic extinctions at the end of the Palaeocene: Nature, v. 353, p. 225–229, https://doi.org/10.1038/353225a0.

Kent, D.V., Cramer, B.S., Lanci, L., Wang, D., Wright, J.D., and Van der Voo, R., 2003, A case for a comet impact trigger for the Paleocene/Eocene thermal maximum and carbon isotope excursion: Earth and Planetary Science Letters, v. 211, p. 13–26, https://doi.org/10.1016/S0012-821X(03)00188-2.

Kineke, G.C., Sternberg, R.W., Trowbridge, J.H., and Geyer, W.R., 1996, Fluid-mud processes on the Amazon continental shelf: Continental Shelf Research, v. 16, p. 667–696, https://doi.org/10.1016/0278-4343(95)00050-X.

Kopp, R.E., Schumann, D., Raub, T.D., Powars, D.S., Godfrey, L.V., Swanson-Hysell, N.L., Maloof, A.C., and Vali, H., 2009, An Appalachian Amazon? Magnetofossil evidence for the development of a tropical river-like system in the mid-Atlantic United States during the Paleocene-Eocene thermal maximum: Paleoceanography, v. 24, PA4211, https://doi.org/10.1029/2009PA001783.

Kuehl, S.A., Allisom, M.A., Goodbred, S.L., and Kudrass, H., 2005, The Ganges–Brahmaputra delta, ***in*** Giosan, L., and Bhattacharya, J.P., eds., River Deltas: Concepts, Models, and Examples: SEPM (Society for Sedimentary Geology) Special Publication 83, p. 413–434, https://doi.org/10.2110/pec.05.83.0413.

Liu, J.P., Kuehl, S.A., Pierce, A.C., Williams, J., Blair, N.E., Harris, C., Aung, D.W., and Aye, Y.Y., 2020, Fate of Ayeyarwady and Thanlwin Rivers sediments in the Andaman Sea and Bay of Bengal: Marine Geology, v. 423, 106137, https://doi.org/10.1016/j.margeo.2020.106137.

Makarova, M., 2018, Application of multiproxy tracers to reconstruct paleoenvironmental perturbations of the mid-Atlantic margin across the Paleocene-Eocene Thermal Maximum [Ph.D. thesis]: New Brunswick, New Jersey, Rutgers University, 205 p.

Makarova, M., Wright, J.D., Miller, K.G., Babila, T.L., Rosenthal, Y., and Park, J.I., 2017, Hydrographic and ecologic implications of foraminiferal stable isotopic response across the U.S. mid-Atlantic continental shelf during the Paleocene-Eocene Thermal Maximum: Paleoceanography, v. 32, p. 56–73, https://doi.org/10.1002/2016PA002985.

McInerney, F.A., and Wing, S.L., 2011, The Paleocene-Eocene Thermal Maximum: A perturbation of carbon cycle, climate, and biosphere with implications for the future: Annual Review of Earth and Planetary Sciences, v. 39, p. 489–516, https://doi.org/10.1146/annurev-earth-040610-133431.

Miller, K.G., Rufolo, S., Sugarman, P.J., Pekar, S.F., Browning, J.V., and Gwynn, D.W., 1997, Early to middle Miocene sequences, systems tracts, and benthic foraminiferal biofacies, New Jersey coastal plain, *in* Miller, K.G., and Snyder, S.W., eds., Proceedings of the Ocean Drilling Program, Scientific Results, Volume 150X: College Station, Texas, Ocean Drilling Program, p. 169–186.

Miller, K.G., et al., 2017, Wilson Lake site, *in* Miller, K.G., Sugarman, P.J., Browning, J.V., et al., Proceedings of the Ocean Drilling Program, Initial Reports, Volume 174AX (Supplement): College Station, Texas, Ocean Drilling Program, https://doi.org/10.2973/odp.proc.174AXS.111.2017.

Nittrouer, C.A., Kuehl, S.A., Sternberg, R.W., Figueiredo, A.G., and Faria, L.E.C., 1995, An introduction to the geological significance of sediment transport and accumulation on the Amazon continental shelf: Marine Geology, v. 125, p. 177–192, https://doi.org/10.1016/0025-3227(95)00075-A.

Röhl, U., Westerhold, T., Bralower, T.J., and Zachos, J.C., 2007, On the duration of the Paleocene-Eocene thermal maximum (PETM): Geochemistry Geophysics Geosystems, v. 8, Q12002, https://doi.org/10.1029/2007GC001784.

Self-Trail, J.M., et al., 2017, Shallow marine response to global climate change during the Paleocene-Eocene Thermal Maximum, Salisbury Embayment, USA: Paleoceanography, v. 32, p. 710–728, https://doi.org/10.1002/2017PA003096.

Stassen, P., Thomas, E., and Speijer, R.P., 2012, Integrated stratigraphy of the Paleocene- Eocene thermal maximum in the New Jersey Coastal Plain: Toward understanding the effects of global warming in a shelf environment: Paleoceanography, v. 27, PA4210, https://doi.org/10.1029/2012PA002323.

Stassen, P., Thomas, E., and Speijer, R.P., 2015, Paleocene–Eocene Thermal Maximum environmental change in the New Jersey Coastal Plain: Benthic foraminiferal biotic events: Marine Micropaleontology, v. 115, p. 1–23, https://doi.org/10.1016/j.marmicro.2014.12.001.

Storms, J.E.A., Hoogendoorn, R.M., Dam, R.A.C., Hoitink, A.J.F., and Kroonenberg, S.B., 2005, Late-Holocene evolution of the Mahakam delta, East Kalimantan, Indonesia: Sedimentary Geology, v. 180, p. 149–166, https://doi.org/10.1016/j.sedgeo.2005.08.003.

Sugarman, P.J., et al., 2010, Medford Site, *in* Miller, K.G., et al., eds., Proceedings of the Ocean Drilling Program, Initial reports, v. 174AX (supplement): College Station, Texas, p. 1–93, https://doi.org/10.2973/odp.proc.ir.174axs.1999.

Trampush, S.M., and Hajek, E.A., 2017, Preserving proxy records in dynamic landscapes: Modeling and examples from the Paleocene-Eocene Thermal Maximum: Geology, v. 45, p. 967–970, https://doi.org/10.1130/G39367.1.

Walsh, J.P., Nittrouer, C.A., Palinkas, C.M., Ogston, A.S., Sternberg, R.W., and Brunskill, G.J., 2004, Clinoform mechanics in the Gulf of Papua, New Guinea: Continental Shelf Research, v. 24, p. 2487–2510, https://doi.org/10.1016/j.csr.2004.07.019.

Wang, H., Wang, J., Chen-Wiegart, Y.K., and Kent, D.V., 2015, Quantified abundance of magnetofossils at the Paleocene-Eocene boundary from synchrotron-based transmission X-ray microscopy: Proceedings of the National Academy of Sciences of the United States of America, v. 112, p. 12,598–12,603, https://doi.org/10.1073/pnas.1517475112.

Wright, J.D., and Schaller, M.F., 2013, Evidence for a rapid release of carbon at the Paleocene- Eocene thermal maximum: Proceedings of the National Academy of Sciences of the United States of America, v. 110, p. 15,908–15,913, https://doi.org/10.1073/pnas.1309188110.

Zachos, J.C., Wara, M.W., Bohaty, S., Delaney, M.L., Petrizzo, M.R., Brill, A., Bralower, T.J., and Premoli-Silva, I., 2003, A transient rise in tropical sea surface temperature during the Paleocene-Eocene Thermal Maximum: Science, v. 302, p. 1551–1554, https://doi.org/10.1126/science.1090110.

Zeebe, R.E., and Lourens, L.J., 2019, Solar System chaos and the Paleocene-Eocene boundary age constrained by geology and astronomy: Science, v. 365, p. 926–929, https://doi.org/10.1126/science.aax0612.

Printed in USA